IIETA International Information and Engineering Technology Association
Advancing the World of Information and Engineering

Journal Européen des Systèmes Automatisés
Vol. 58, No. 12, December, 2025, pp. 2585-2591
Journal homepage: http://iieta.org/journals/jesa

Optimal and Robust FOPID Controller for Overhead Cranes Systems Based PSO

Jasim Khalaf*, Ali Mary, Ahmad Al-Talabi

Department of Mechatronics Engineering, Khwarizmi College of Engineering, University of Baghdad, Baghdad 10071, Iraq

Corresponding Author Email: jassem.khalaf2402m@kecbu.uobaghdad.edu.iq

https://doi.org/10.18280/jesa.581211

Received: 13 August 2025
Revised: 18 November 2025
Accepted: 28 November 2025
Available online: 31 December 2025

Keywords:
FOPID, optimal control, overhead crane system

ABSTRACT

Recently, the Fraction Order PID (FOPID) used widely instead of the traditional proportional-integral-derivative (PID) due to its important advantages, including simple structure, good tracking, high robustness against external disturbance, and its ability to handle the parameters variations and high nonlinear in the dynamic model of the systems. This paper aims to design an optimal robust control method with a good trade-off between the transient response specifications and high robustness against external disturbance and system uncertainty. To achieve this aim, multi-objective optimization-based particle swarm optimization (PSO) has been used to tune the gain parameters of the FOPID. The fractional parameters of the FOPID add flexibility to tune the response of the dynamic system. A new composite objective function has been used to ensure minimum swing with good tracking. Selecting suitable values for the weighting function in the objective function represent an important step in the proposed control method. The simulations are carried out for the presented controller and the results are compared with several controllers. The simulation results illustrated superior performance of the suggested controller with good transient's specifications and high robustness against external disturbance.

1. INTRODUCTION

Overhead cranes serve as vital infrastructure in today's industrial settings, allowing for the movement of very large loads in all three spatial dimensions while also increasing safety and productivity within operations [1, 2]. Overhead cranes, considered mechanical systems, are largely used in production facilities, distribution centers, shipyards, and warehouses—a common trait across these settings is the way that these systems can move loads as controlled three-dimensional motion. The ease or ability to control three-dimensional motion of loads can significantly affect overall productivity and worker safety. At the same time, the operation and control of overhead crane systems represent a significant technical challenge because of its structure. Most phenomena of motion of an overhead crane constitute underactuated mechanical systems—in which the number of control inputs is less than the total number of degrees of freedom for the system [1, 3]. The primary control objectives will remain the same in industrial settings or applications: the achievement of precise positioning, the inhibition of payload sway during motion, and the rejection of disturbances during operation. Historically, crane systems have been controlled using techniques founded on the proportional-integral-derivative (PID) control architecture. Because they are simple to implement, relatively low-computational, and have established tuning rules, traditional PID controllers are still largely used in industrial practice [4, 5]. However, the fixed gain properties of conventional PID controllers limit their capabilities to handle the sometimes-extreme nonlinear dynamics often inherent in underactuated tap systems. Recent work has shown that using meta-heuristic optimization methods, and in particular particle swarm optimization (PSO) algorithms, can mitigate oscillations through explicit tuning of the PID control gain to stabilize payload motion [4]. Model predictive control is a significant advancement in overhead crane control theory, and represents significant theoretical and practical advantages to enable the simultaneous objectives of load stabilization and damp vibrations [1]. Specifically, the MPC framework gives users the ability to move the ball overhead crane system multiple axes in a coordinated motion while minimizing payload oscillations by physically constraining the controller formulation, optimizing over a limited prediction horizon, and systematically predicting future system dynamics for optimal control inputs. Fuzzy Logic Control has arisen as a potent approach for addressing uncertainty and nonlinearities that characterize crane systems that operate under variable load and varying conditions [6]. It has been shown through both simulation and experimental work that hybrid-type control structures that use fuzzy logic with known proportional-integral-derivative control (i.e., fuzzy-PID control) have significantly improved swing suppression capabilities better than traditional PID or pure fuzzy control strategies [7]. Sliding Mode Control techniques have been shown as a robust control methodology for many complex system systems like robotic and crane system with significant external disturbance and model uncertainty [8, 9]. The theoretical merits of SMC, including guaranteed finite-

time convergence, less sensitivity to parameter change, and insensitivity to matched external disturbances, have led to authors turning their work toward creating advanced forms that specifically match the conditions of crane systems [10, 11]. Nonlinear, adaptive and fractional-order sliding mode controllers have demonstrated to be very effective managing dynamic and multi-degree-of-freedom crane system models [12, 13]. Recently, there has been extensive research interest in hybrid control architectures, which automatically combine multiple control methodologies. Hybrid control architectures utilizing sliding mode controller mechanisms with PID logic take advantage of the disturbance rejection properties of SMC while preserving the simplicity of implementation [14]. Control systems that incorporate a neural network have proven to outperform PID methods in simultaneous system stability and robustness, as well as oscillation suppression, during dynamic crane motion [15]. In the study [16], a state space fuzzy controller used to represent the nonlinear dynamic of the crane system with the linear-matrix-inequality A Takagi-Sugeno fuzzy control with Input Shaping method are combined to reduce the swing by representing the nonlinear system as a sub system for different operating points [17]. Although, most these presented achieved good performance but in practical, there are many difficulties in implementing these controller. In this paper, FOPID controller with multi object function based PSO algorithm has been suggested. The main contribution of his paper is; use FOPID controller for the crane system, which provide more flexibility and high robustness with respect to PID controller Multi objective optimization technique based PSO has been used to tune the parameter s of the FOPID ensuring good tracking performance with high robust against external disturbance and system uncertainty by selecting suitable weighting function for each term used in the cost function. A novel multi-objective function is designed that taking into account the accuracy, sway angle elimination, transient specifications, and robustness. This proposed performance index is expected to give superior result comparing with the standard performance index like IAE, ITAE, or ISE. Examine the performance of the proposed controller in several cases to check its performance and robustness and compare its results with other standard controllers.

2. THE DYNAMIC EQUATIONS OF MOTION OF AN OVERHEAD CRANE SYSTEM

The mathematical model representing the overhead crane system was derived using the Lagrange equation. The equations of motion were obtained from the free body diagram of the system [18]. One of the benefits of the Lagrange approach is that it is able to fully account for kinetic and potential energies and thus provides a systematic way to derive nonlinear dynamics [19, 20].

The system consists of a cart of mass M and a payload of mass m attached to the trolley. The total kinetic energy is:

$$T = \frac{1}{2}M\dot{x}^2 + \frac{1}{2}m(\dot{x}^2 + \dot{z}^2) \tag{1}$$

The potential energy:

$$U = mgz = mgL(1 - \cos\theta) \tag{2}$$

where, x: Horizontal displacement of the cart, $Z = L(1 - \cos\ \theta)$ Vertical displacement of the payload center of mass, L: Length of the payload, θ: Angle of the payload, M: Mass of the trolley, m: Mass of the payload. The Lagrangian is the difference between kinetic and potential energy:

$$\begin{gathered} L = T - U \\ L = \frac{1}{2}(M+m)\dot{x}^2 + \frac{1}{2}mL^2\dot{\theta}^2 \\ +mL\dot{x}\dot{\theta}\cos\ \theta - mgL(1 - \cos\ \theta) \end{gathered} \tag{3}$$

The equations of Motion can be obtained using the Euler-Lagrange equation:

$$\frac{d}{dt}\left(\frac{\partial L}{\partial \dot{q}}\right) - \frac{\partial L}{\partial q} = 0 \tag{4}$$

$$(M+m)\ddot{x} + mL\ddot{\theta}\cos\ \theta - mL\dot{\theta}^2\sin\ \theta = F \tag{5}$$

$$mL\ddot{x}\cos\ \theta + mL^2\ddot{\theta} + mgL\sin\ \theta = 0 \tag{6}$$

2.1 Dynamic model linearization

To linearize the dynamic model of the crane system, the oscillations assume to be small ($\theta \rightarrow 0$):

$$\sin\ \theta \approx \theta, \cos\ \theta \approx 1, \dot{\theta}^2 \rightarrow 0$$

The equations become:

$$\begin{gathered} (M+m)\ddot{x} - mL\ddot{\theta} = F \\ mL\ddot{x} + mL^2\ddot{\theta} + mgL\theta = 0 \end{gathered} \tag{7}$$

To express the system in state space, define the state vector:

$$\mathbf{x} = \begin{bmatrix} x \\ \theta \\ \dot{x} \\ \dot{\theta} \end{bmatrix} \tag{8}$$

The state-space equations are:

$$\begin{gathered} \dot{\mathbf{x}} = A\mathbf{x} + Bu \\ y = C\mathbf{x} + Du \end{gathered} \tag{9}$$

State-Space Matrices:

$$\begin{gathered} A = \begin{bmatrix} 0 & 0 & 1 & 0 \\ 0 & 0 & 0 & 1 \\ 0 & \frac{mg}{M} & 0 & 0 \\ 0 & -\frac{g(M+m)}{ML} & 0 & 0 \end{bmatrix}, B = \begin{bmatrix} 0 \\ 0 \\ \frac{1}{M} \\ -\frac{1}{ML} \end{bmatrix} \\ C = \begin{bmatrix} 1 & 0 & 0 & 0 \\ 0 & 1 & 0 & 0 \end{bmatrix}, D = \begin{bmatrix} 0 \\ 0 \end{bmatrix} \end{gathered} \tag{10}$$

3. PROPOSED CONTROL METHOD AND OPTIMIZATION ALGORITHMS

This section investigates the two objective that represents the core of this research. Design a FOPID controller for the Overhead cranes systems, then improving the performance of FOPID controller by using optimization algorithm to tune their

gain values.

3.1 FOPID controller design

This section discusses the FOPID, which is represents, an improved version of the standard PID controller. In addition to the three standard parameters of the PID (K_p, K_i, and K_d), two parameters had been added (λ, μ). The control law of FOPID controller can be expressed as follows:

$$u(t) = K_p e(t) + K_i \frac{d^{-\lambda}}{dt^{-\lambda}} e(t) + K_d \frac{d^{\mu}}{dt^{\mu}} e(t) \tag{11}$$

where, *e(t)* refers to the difference between the desired response and the measured response. Figures 1 and 2 shows implementation of the proposed control law. The important challenge in this design is how select the gain values of the FOPID to achieve optimal performance. Thus, PSO optimization algorithm had been used to tune these parameters.

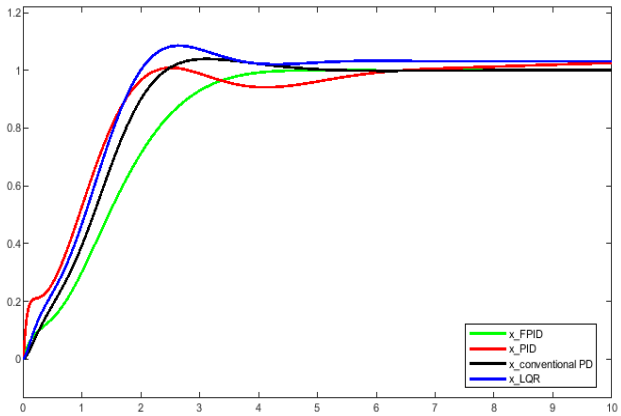

Figure 1. Step response for cart position

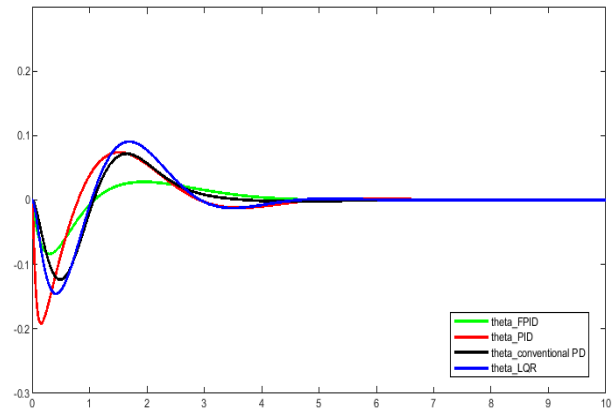

Figure 2. Step response for payload angle (θ)

3.2 Multi-objective optimization problem

To adjust the gains of the Fractional-Order PID (FOID) controller based on the developed dynamic model of the overhead crane system, PSO was used. In this optimization procedure, PSO will augment an initial swarm of particles in the search space, where particles denote feasible solutions. The position and velocity of particles as matrices are defined by the dimension of the swarm size, or total number of particles used in the search. The position and velocity of each particle are updated according to the following formulas:

$$v_i(t+1) = wv_i(t) + c_1 r_1\left(p_i{}^{best} - x_i(t)\right) + c_2 r_2\left(g^{best} - x_i(t)\right) \tag{12}$$

$$x_i(t+1) = x_i(t) + v_i(t+1) \tag{13}$$

where, v_i and x_i represent the velocity and position of particle at iteration *i*. c_1 and c_2 denote Cognitive and Social coefficients respectively. w is Inertia weight. r_1 and r_2 are random numbers. $p_i{}^{best}$ represents the best position of particle *i*. g^{best} denotes the global best position. As the algorithm iteratively updates the position and velocity of particles, encouraging an optimal set of controller parameters that generate improvements to the system's performance, the goal becomes to minimize a performance index in the time domain, leading to a faster and more stable system response behavior. The FPID feedback controller developed is designed to ensure that the cart reaches its required final position while minimizing the swing angle of the payload, thereby improving the stability and responsiveness of the overhead crane system, the following optative function used for tuning the gain parameters of the FOPID:

$$j = \sum_{i=1}^{5} w_i f_i \tag{14}$$

where, w_i denotes the *i*-th weighting function and f_i represent the i-th objective function where i = 1,2,3,4,5.

$$f_1 = \int_0^{tf} te(t)dt \tag{15}$$

This objective function denotes the integral time square error aims to minimize the difference between desired reference and the measured output.

$$f_2 = SS \tag{16}$$

This objective function tries to minimize Steady-State used to penalize deviations from the final desired values.

$$f_3 = M_p \tag{17}$$

This objective function tries to minimize the overshot to ensure minimum deviation from the desired reference.

$$f_4 = OSC \tag{18}$$

This function minimizes the oscillation magnitude system to reduce undesirable vibrations in the system.

$$f_5 = \int \|T_{zw}(s)\|_\infty \, dw \tag{19}$$

This function is H_∞ (H-infinity) norm. $\|T_{zw}(s)\|$ represents the transfer function from the disturbance to the output.

$$\|T_{zw}(s)\|_\infty \stackrel{\text{def}}{=} \sup \sigma(T_{zw}(jw)) \tag{20}$$

The H_∞ refers to the maximum possible gain of the controlled system from the disturbance signal to the performance output over all frequencies.

4. SIMULATION RESULTS

A full simulation of the anti-swing underactuated crane system was conducted in MATLAB 2018 to evaluate the performance and robustness of several linear control strategies. The focus was on four controllers; the FOPID ontroller, the PID controller, conventional PD controller, and Linear Quadratic Regulator (LQR) controller. The performance of all controllers was considered in terms of the ability to suppress payload oscillation given system uncertainties and external disturbances. Thus, in order for all proposed controllers to perform optimally, the parameters for all controllers were tuned by utilizing the PSO algorithm. For the PSO, the weighting functions selected as follows; $w_1 = 20$, $w_2 = 41$, $w_3 = 30$, $w_4 = 20$, $w_5 = 15$. The optimized parameters for all controllers (FOPID, PID, conventional PD, and LQR) are summarized in Tables 1, 2, 3 and 4 respectively.

Table 1. Parameters for theta and position for fractional PID controller

Parameter	FPID for Position (x)	FPID for Theta (θ)
Kp	3	13.0015
Ki	1	60
λ (lambda)	0.1	1.0265
Kd	1	14.8541
μ (mu)	1.1	0.92171

Table 2. Parameters for theta and position for PID controller

Parameter	PID for Position (x)	PID for Theta (θ)
Kp	2.4378	30
Ki	0.1	30
Kd	7.0626	24.7642

Table 3. Parameters for theta analog controller and position for PD controller

Controller	Parameter	Value
PD Controller (Position x)	Kp	2.04398191768923e+07
	Kd	2.04145787076263
State -Space Controller (Angle θ)	A	[775502, 24.8960] [-49.8611, -64.9887]
	B	[-102.6676] [79.8933]
	C	[-30.0323, 9.0762]
	D	39.6711

Table 4. LQR controller parameters

Controller	Parameter	Value
LQR Controller	K (Gain Vector)	[31.9952, -95.5307, 31.9949, -9.4619]

4.1 Step reference tracking

This study examined the response of an underactuated overhead crane following a unit step input using FOPID, PID, classical PD and LQR pseudo-control laws. Each pseudo-control law was evaluated based on time response characteristics, which includes settling time, rise time, overshoot and Integral Absolute Error (IAE). Figures 1 and 2 include the time response plots with the reference input tracked successfully by all control laws. The pseudo-control laws had distinct transient responses in terms of settling time, rise time, overshoot, and IAE. Regarding x (cart position) tracking behavior; the FOPID and PID showed reference tracking characteristics of 0% overshoot and were able to smoothly track the reference input (Figure 1). The LQR controller produced a small 5.31% overshoot for x, in comparison to 3.95% for the PD controller (Table 5). In terms of settling time, FOPID and LQR controllers performed similarly with settling time of 3.65 s and 3.33 s respectively; and the settling time of PID and PD was 6.90 s and 4.11 s respectively. The rise time was relatively similar, with LQR (1.60 s) and PID (1.78 s) both being quicker than FOPID (2.51 s) and PD was similar (1.73 s).

Table 5. Transient specifications for cart position (x) for nominal case

Controller	Rise Time (s)	Settling Time (s)	Overshoot (%)
FPID	2.5112	3.6537	0
PID	1.7782	6.8971	0
LQR	1.6031	3.3289	5.3128
conventional PD	1.7291	4.1138	3.9542

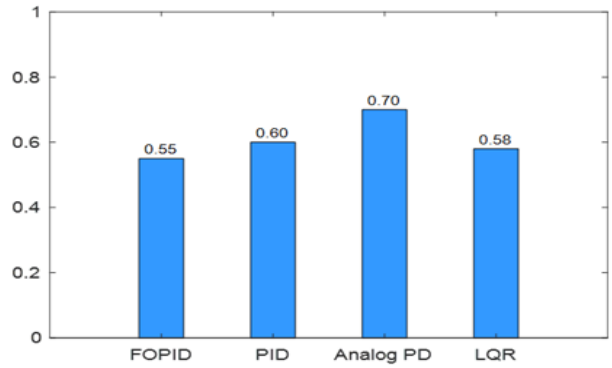

Figure 3. IAE values for cart position (x)

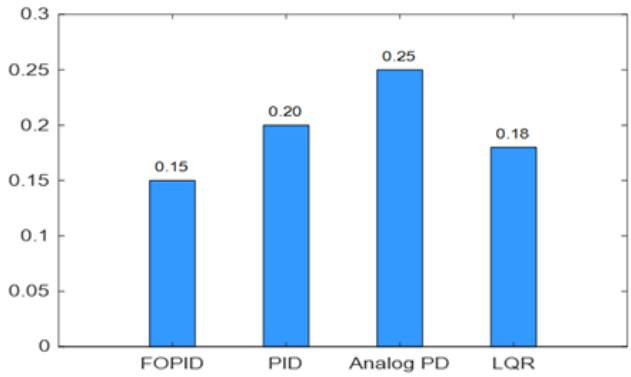

Figure 4. IAE values for each controller for payload angle (θ)

The IAE values for cart position presented in Figure 3 also affirm the transient results. In the cart position, the values recorded by the FOPID controller were the lowest IAE recorded at IAE = 0.55, while LQR had the second lowest IAE of IAE = 0.58, as these were the only controllers to have IAE below 1.00 indicating considerable precision and extent of minimized error. The IAE value the PID controller recorded was IAE = 0.78 and the PD controller had the highest IAE at IAE = 1.08 which corroborate its overshoot and the damping characteristics that were less than the other controllers. The controllers were rated as well based on the controlled angle (θ)

of the swing payload. Figure 4 depicts the swings angle IAE of the four controllers, where the FOPID controller once again was victorious again with an IAE of 0.15, LQR produced an IAE of 0.18, PID with an IAE of 0.20, and the PD controller had the highest IAE at 0.25. The entire dynamic responses are reported in Table 6. While the PD controller showed the fastest settling time of 3.42 s, this controller produced notable excessive oscillations at the peak overshoot (5.28×10^{6}%) and undershoot (3.08×10^{6}%). While the FOPID had the second highest settling time of 4.46 s, with a rise time of 8.21×10^{-5} s, the FOPID controller produced a modest peak (0.0837) and demonstrably controlled very stable angular motion with extremely small deviations. To sum this up, the FOPID controller exhibited superior control performance in all cases with high stability and low overshoot, converged swiftly and stably, while minimizing the IAE values for both cart position and swing payload angle and the preference of FOPID was supported by the results of the experimentation. The nominal parameters of the crane system are as follows: m = 1 kg, M = 2 kg, L = 1 m and g = 9.81 m/s^2.

Table 6. Transient specifications for payload angle (θ) for nominal case

Controller	Rise Time (s)	Settling Time (s)	Overshoot (%)	Peak Value	Peak Time (s)
FPID	8.2068e-05	4.4584	3.4894e+05	0.0837	0.2915
PID	7.8100e-04	4.5387	3.3145e+04	0.1917	0.1533
LQR	6.2401e-04	4.3366	1.8221e+06	0.1458	0.4172
conventional PD	4.7738e-04	3.4198	5.2783e+06	0.1236	0.4722

4.2 Disturbance rejection

A disturbance signal with amplitude 1 was applied at t = 6.5 seconds to investigate the robustness of all controllers. The cart position and payload angles of the controllers during applied the disturbance are shown in the figures. These figures show that all the controllers had been affected with disturbance but this disturbance partially recovered by the controllers. It can be seen form these figures, that the FOPID recover the cart position and payload angle smoothly and quickly with minimum oscillation which mean tis more robustness against the external disturbance. The results presented in Figures 5 and 6.

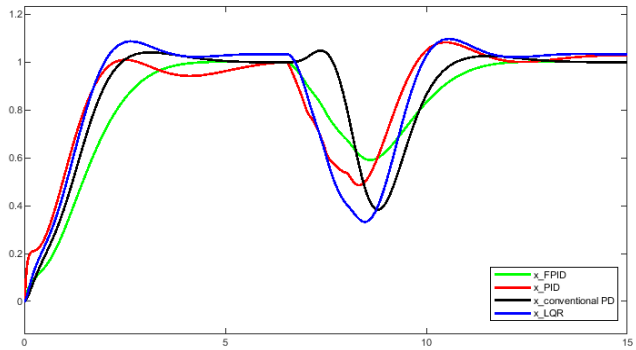

Figure 5. Response cart position (x) for disturbance

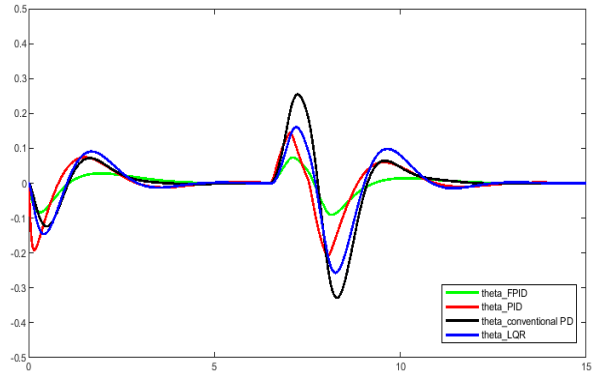

Figure 6. Response payload angle (θ) for disturbance

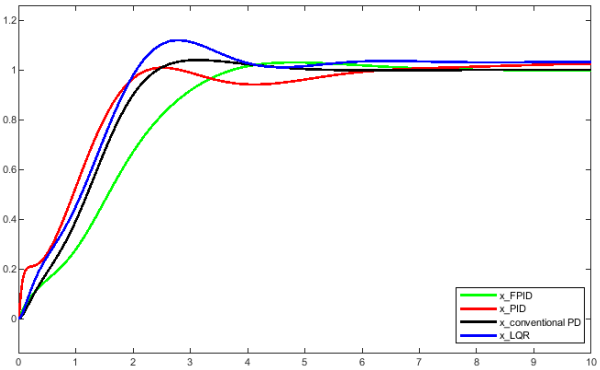

Figure 7. Response cart position (x) for uncertainty

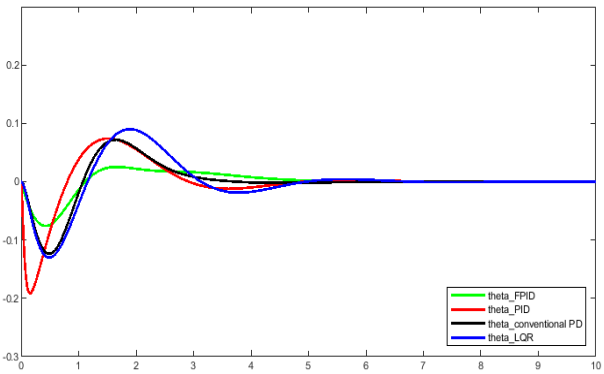

Figure 8. Response payload angle (θ) for uncertainty

4.3 System uncertainty

To analyze the robustness of the proposed control methodologies to apply changes to the crane system parameters from their nominal values. An example of this would be to apply real-world unexpected phenomena that cause difficulties from modeling errors, external disturbances, or changes in parameters. The mass of the pendulum was changed to $m = 1.3$ kg, the mass of the cart was changed to $M = 2.6$ kg, the pendulum length was changed to $L = 1.4$ m, and the gravitational acceleration was kept at $g = 9.81$ m/s^2. The new values resulted in new state-space matrices that were derived from the linearized equations to use the system with the unknown factors that could influence its behavior with time. The results of the simulations depicted in Figures 7 and 8 show that all proposed controllers, especially the FOPID controller maintain a stable and acceptable response to a system with defined system parameters after changing the initial parameter

values. The transient response results for the cart position and pendulum angle were summarized in Tables 7 and 8, and exemplified the robustness of the FOPID controller with respect to conventional PID, LQR, and conventional PD controllers. The FOPID controller can achieve acceptable rise time, settling time, and overshoot compared to the other controllers, and therefore can be concluded that the FOPID controller is efficient under uncertain operation conditions.

Table 7. Transient specifications for cart position (x) for uncertainty case

Controller	Rise Time (s)	Settling Time (s)	Overshoot (%)	Peak	Peak Time (s)
FPID	2.6395	5.8967	3.0413	1.03	4.8552
PID	1.9858	6.722	0	1.0289	10
LQR	1.6846	4.7099	8.4548	1.1187	2.7177
conventional PD	1.7299	4.1141	3.9567	1.0396	3.1753

Table 8. Transient specifications for payload angle (θ) for uncertainty case

Controller	Rise Time (s)	Settling Time (s)	Overshoot (%)	Peak	Peak Time (s)
FPID	0.0011318	5.1847	26.690	0.025425	1.6612
PID	0.00029069	4.5278	89.198	0.07416	1.5534
LQR	0.0046369	6.2317	55.834	0.090285	1.8768
conventional PD	0.00011524	3.4164	206.120	0.072186	1.6612

5. CONCLUSIONS

The research presented in this paper is a comprehensive comparative study of linear control strategies for anti-swing control in underactuated overhead crane systems, including a FOPID controller, a standard PID, an analog PD, and a LQR controller proposed in this work and optimized using PSO. The testing shows that the FOPID controller performed best in all our metrics, including reaching the least Integral Absolute Error (IAE = 0.55), no overshoot in nominal conditions, and showing the highest robustness to external disturbances and parameter uncertainty within the parameters prescribed in this paper. The FOPID controller's framework in fractional-order calculus allows an enhanced tuning capability with two additional tuning parameters (λ and μ), and can be tuned using nonlinear crane dynamics much more easily than the conventional controllers that are static in the left-hand plane. In particular, within the disturbance rejection and system uncertainty conditions, the FOPID showed stable performance in nominal conditions with only a slight degradation in performance, while the other controllers showed varying degrees of performance degradation. In conclusion, the FOPID controller is the right candidate for real-world applications of overhead cranes operating under precision positioning and swing take down of the payload, and importantly makes an important contribution towards the controlling of underactuated mechanical systems and also lays a fundamental framework for future exploration of more advanced crane control and uses in automation systems in industry.

ACKNOWLEDGMENT

This work was supported by the Department of Mechatronics Engineering, Al-Khwarizmi College of Engineering, University of Baghdad, Iraq.

REFERENCES

[1] Khanh, H.B.T., Thi, M.H., Hue, L.T., Nguyen, T.L., Nguyen, D.H. (2024). Flatness-based motion planning and model predictive control of industrial cranes. Engineering Technology & Applied Science Research, 14(4): 15141-15148. https://doi.org/10.48084/etasr.7662

[2] Yang, M., Xu, W. (2025). Adaptive time delay estimation and dynamic residual-assisted prescribed performance control of overhead crane systems based on a fractional-order ultra-local model. Journal of the Franklin Institute, 362(18): 108203. https://doi.org/10.1016/j.jfranklin.2025.108203.

[3] Miranda-Colorado, R., Rodríguez-Arellano, J.A., Aguilar, L.T. (2025). Control of a 2D-crane system with payload swing attenuation: An observer-based prescribed-time approach. Applied Mathematical Modelling, 147: 116226. https://doi.org/10.1016/j.apm.2025.116226

[4] Azmi, N.I.M., Yahya, N.M., Fu, H.J. Yusoff, W.A.W. (2019). Optimization of the PID-PD parameters of the overhead crane control system by using PSO algorithm. MATEC Web of Conferences, 255: 04001. https://doi.org/10.1051/matecconf/201925504001

[5] Mary, A.H., Miry, A.H., Miry, M.H. (2022). Design robust H∞-PID controller for a helicopter system using sequential quadratic programming algorithm. Journal of the Chinese Institute of Engineers, 45(8): 688-696. https://doi.org/10.1080/02533839.2022.2126401

[6] Sun, Z., Ling, Y.W., Tan, X., Zhou, Y., Sun, Z.X. (2021). Designing and application of type-2 fuzzy PID control for overhead crane systems. International Journal of Intelligent Robotics and Applications, 5: 10-22. https://doi.org/10.1007/s41315-020-00157-w

[7] Jaafar, H.I., Mohamed, Z., Mohd Subha, N.A., Husain, A.R., Ismail, F.S., Ramli, L., Tokhi, M.O., Shamsudin, M.A. (2018). Efficient control of a nonlinear double-pendulum overhead crane with sensorless payload motion using an improved PSO-tuned PID controller. Journal of Vibration and Control, 25(4): 907-921. https://doi.org/10.1177/1077546318804319

[8] Ahmed, M.S., Mary, A.H.M., Jasim, H.H. (2021). Robust computed torque control for uncertain robotic manipulators. Al-Khwarizmi Engineering Journal, 17(3): 22-28. https://doi.org/10.22153/kej.2021.09.002

[9] Zheng, S., Ouyang, H. (2022). Adaptive fuzzy tracking control for vibration suppression of tower crane with distributed payload mass. Automation in Construction,

142: 104521. https://doi.org/10.1016/j.autcon.2022.104521
[10] Zhang, J.Y., Wu, W., Huang, X. (2024). Robust sliding-mode control for a gantry crane system subject to external disturbance. Nonlinear Dynamics, 112: 4599-4615. https://doi.org/10.1007/s11071-024-09294-4
[11] Mary, A., Miry, A., Miry, M. (2019). Mixed robust controller with optimized weighted selection for a DC servo motor. In Proceedings of the International Conference on Information and Communication Technology, Baghdad, Iraq, pp. 178-183. https://doi.org/10.1145/3321289.3321304
[12] Spruogis, B., Jakstas, A., Gican, V., Turla, V. Moksin, V. (2018). Further research on an anti-swing control system for overhead cranes. Engineering Technology & Applied Science Research, 8(1): 2598-2603. https://doi.org/10.48084/etasr.1774
[13] Zhang, F., Geng, J., Chen, Z., Zhou, L., Shao, X., Zhang, J. (2024). Fractional-order sliding mode control for a container crane system. In 2024 14th Asian Control Conference (ASCC), Dalian, China, pp.1-6.
[14] Antic, D., Jovanovic, Z., Peric, S., Nikolic, S., Milojkovic, M., Milosevic, M. (2012). Anti-swing fuzzy controller applied in a 3D crane system. Engineering Technology & Applied Science Research, 2(2): 196-200. https://doi.org/10.48084/etasr.146
[15] Mary, A.H., Miry, A.H., Kara, T., Miry, M.H. (2021). Nonlinear state feedback controller combined with RBF for nonlinear underactuated overhead crane system. Journal of Engineering Research, 9(3): 197-208. https://doi.org/10.36909/jer.v9i3A.9159
[16] Aguiar, C., Leite, D., Pereira, D., Andonovski, G., Škrjanc, I. (2021). Nonlinear modeling and robust LMI fuzzy control of overhead crane systems. Journal of the Franklin Institute, 358(2): 1376-1402. https://doi.org/10.1016/j.jfranklin.2020.12.003
[17] Nguyen, H.P., Bui, N.T., Nguyen, T.V.A. (2024). Tracking control based on Takagi–Sugeno fuzzy descriptor model for overhead crane combined with input shaping. IEEE Access, 12: 127507-127521. https://doi.org/10.1109/ACCESS.2024.3456815
[18] Kim, T.D., Nguyen, T.N., Do, D.M., Le, H.X. (2022). Adaptive neural network hierarchical sliding mode control for six degrees of freedom overhead crane. Asian Journal of Control, 25(4): 2736-2751. https://doi.org/10.1002/asjc.2961
[19] Li, G., Ma, X., Li, Z., Li, Y. (2021). A Nonlinear coupling-based motion trajectory planning method for double-pendulum rotary crane subject to state constraints. In The International Conference on Applied Nonlinear Dynamics, Vibration and Control, pp. 168-183. https://doi.org/10.1007/978-981-16-5912-6_13
[20] Cecotti, S. (2024). From Newtonian dynamics to Lagrangian mechanics. In Analytical Mechanics. UNITEXT for Physics, pp. 3-22. https://doi.org/10.1007/978-3-031-59264-5_1

NOMENCLATURE

M	The mass of the cart, kg
m	Mass of payload, kg
L	Length of the payload
g	Gravitational constant, m/s^2
X	Horizontal displacement of the cart.m
Z	Vertical displacement of the payload center of mass.m
θ	angle of the payload.rad
F	the Horizontal force on cart
T	kinetic energy
U	potential energy
L = T-U	The Lagrangian is the difference between kinetic and potential energy

Greek symbols

μ	parameter of fractional FOPID
λ	parameter of fractional FOPID